Untangling the Waves: Decomposing Extreme Sea Levels in a non-tidal basin, the Baltic Sea

Marvin Lorenz[1,2], Katri Viigand[3], and Ulf Gräwe[1]

[1]Leibniz Institute for Baltic Sea Research Warnemünde, Rostock, Germany
[2]Federal Waterways Engineering and Research Institute, Hamburg, Germany
[3]Department of Cybernetics, School of Science, Tallinn University of Technology, Tallinn, Estonia

Correspondence: Marvin Lorenz (marvin.lorenz@io-warnemuende.de)

Abstract. Extreme sea level (ESL) events are typically caused by the combination of various long surface waves, such as storm surges and high tides. In the non-tidal, semi-enclosed Baltic Sea, however, ESL dynamics differ. Key contributors include the Baltic's variable filling state (preconditioning) due to limited water exchange with the North Sea and inertial surface waves, known as seiches, which are triggered by wind, atmospheric pressure, and basin bathymetry. This study decomposes ESL events in the Baltic Sea into three key components: the filling state, seiches, and storm surges. Our results show that storm surges dominate the western Baltic, while the filling state is more influential in the central and northern regions. Using a numerical hydrodynamic model, we further decompose these components based on their driving forces: wind, atmospheric pressure, North Atlantic sea level, baroclinicity, and sea ice. Wind and atmospheric pressure are the primary forces across all components, with the Atlantic sea level contributing up to 10% to the filling state. These findings offer a deeper understanding of ESL formation in the Baltic Sea, providing critical insights for coastal flood risk assessment in this unique region.

1 Introduction

The threat of extreme sea level (ESL) events escalates along the world's coastlines due to the rising mean sea level. This phenomenon is a leading cause of flooding in coastal areas, affecting more than 100,000 people annually in Europe alone. Moreover, this number is projected to rise in the future (Vousdoukas et al., 2020). Due to anthropogenic climate change, ESLs are projected to increase not only due to the rising mean sea level (e.g. Fox-Kemper et al., 2021), but also due to the intensification of tropical storms (e.g. Knutson et al., 2010) and changing sea level dynamics due to sea level rise (e.g. Moftakhari et al., 2024), such as increasing tidal amplitudes and surges in estuaries (e.g. McGranahan et al., 2007; Talke et al., 2021) or coastal lagoons (e.g. Bilskie et al., 2014; Lorenz et al., 2023).

ESLs are often a combination of several processes, each leading to an increase in coastal sea level, e.g. high tides, storm surges, wave setup due to breaking wind waves, river discharge, and other surface waves. Storm surges occurring at high tide are the most common cause of ESLs for most coastal areas. For estuaries, where rivers flow into the sea, the coincidence of a storm surge at high tide with extreme river discharge poses a major flood hazard (e.g. Wahl et al., 2015; Hendry et al., 2019). Generally, when two or more extreme events co-occur, they are called compound events. Since many different components can contribute to ESLs, it is desirable to understand and quantify each to assess each contributor's risk and statistics. However,

25 decomposing ESLs is challenging. Using tide gauges alone, only a temporal decomposition is possible, e.g. the separation of tides and surges. However, non-linear interactions between the two complicate the separation (Idier et al., 2019; Arns et al., 2020) and are, as a result, often neglected in impact studies (e.g. Rueda et al., 2017; Vousdoukas et al., 2018; Kirezci et al., 2020). Numerical models can allow the decomposition of ESL events into their different contributions, as individual processes and forcings can be switched on or off (Parker et al., 2023). In this way, each contributor can be quantified. Numerical models

30 rely on good input data, such as atmospheric forcing with a good representation of storm systems, to capture storm surges and, hence ESLs correctly. However, long-term, high-quality, high-resolution reanalysis data that meet these requirements are often not available. Therefore, models are not always able to reproduce every individual event accurately. Nevertheless, comparison with tide gauge data has shown that models can still correctly reproduce ESL statistics. Therefore, models are invaluable for decomposing ESL events into different components and forcings. Most decomposition studies assume a linear superposition of

35 the individual sea level contributors (e.g. Parker et al., 2023). Interactions between the different contributors are often attributed to a residual term.

In this study, we follow the decomposition approach to analyse the ESLs within a non-tidal, semi-enclosed marginal sea, the Baltic Sea (Fig. 1). The Baltic Sea, located in northern Europe, has a mean depth of approximately 55 m. The region experiences postglacial isostatic land uplift of about 10 mm/year in the northern part of the sea, while the very southern region

40 experiences subsidence of about 0.05 mm/year (Vestøl et al., 2019). Long-term global eustatic sea level rise in the Baltic Sea is not uniformly distributed across the region. It varies from 2 mm/year in the western part of the sea to more than 5 mm/year in the Gulf of Bothnia. About 75% of the basin-averaged sea level rise can be attributed to the external sea level signal while intensifying winds and poleward shifting low-pressure systems explain the spatial variation in the mean sea level trends (Gräwe et al., 2019). The prevailing winds are westerly to southerly (Bierstedt et al., 2015) and ESLs usually occur in autumn

45 and winter when storm systems pass over the Baltic Sea region. A series of clustered storm systems can cause exceptionally high ESLs in the northern Baltic Sea due to the overlapping effects of previous storms (Rantanen et al., 2024). In the Western Baltic Sea, very high sea levels have been observed in recent years (Groll et al., 2024), including the highest sea levels since 1872 in October 2023 (Kiesel et al., 2024). Events like these cause flooding, which will become more severe with sea level rise (Kiesel et al., 2023b) and pose problems for current flood protection in the future (Kiesel et al., 2023a).

50 A recent review of the sea level dynamics and ESL events in the Baltic Sea has been compiled by Weisse et al. (2021) and Rutgersson et al. (2022) as part of the Baltic Earth Assessment Reports (BEARs). The sea level dynamics and the ESLs of the Baltic Sea have some unique contributions that distinguish the dynamics of the Baltic Sea from other coasts around the globe. First, the Baltic Sea has negligible tides (e.g. Gräwe and Burchard, 2012). In addition, since the Baltic Sea is separated from the North Sea by the shallow and narrow Danish Straits, water exchange between the Baltic Sea basin and the North Sea is

55 hindered. The Danish Straits effectively act as a low-pass filter, filtering out high-frequency surface waves, such as storm surges and tides from the North Sea. On the other hand, the slow water exchange on a time scale of a week and longer determines the mean sea level of the Baltic Sea, also called the *filling* state or, in the context of ESL events, the *preconditioning* (Leppäranta and Myrberg, 2009; Madsen et al., 2015). This exchange is mainly controlled by the westerly winds (Gräwe et al., 2019). Similarly, local preconditioning in sub-basins can contribute to ESLs, e.g. up to 1 m in the Gulf of Riga (Männikus et al.,

2019). Although the Baltic Sea has negligible tides, there are basin-wide inertial surface waves with fixed frequencies between $(13\,\text{h})^{-1}$ and $(44\,\text{h})^{-1}$ which are given by the basin geometry (e.g. Wübber and Krauss, 1979; Zakharchuk et al., 2021). These inertial waves are called *seiches* and are excited by perturbations in the sea level. Their amplitudes can be as large as 17 cm, although their initial perturbations were smaller (Zakharchuk et al., 2021). Together with *storm surges*, these three temporal components (filling, seiches and storm surges) are the main contributors to ESL events. At the coast, local sea levels may be directly elevated by wind-driven wave effects, such as wave setup (Su et al., 2024) or wave run-up. Meteotsunamis can be an additional component (Pellikka et al., 2020, 2022). Due to local geometries and orientations of the coastal topography, different regions are susceptible to different combinations of compounding contributions. Therefore, the return levels of ESLs are very heterogeneous. The return levels for a 30-year ESL event range from 0.7 to 2.5 m above mean sea level (Lorenz and Gräwe, 2023a), with the highest ESLs occurring at the head of the Gulf of Finland, the Gulf of Riga, and in the Western Baltic Sea (Wolski et al., 2014; Wolski and Wiśniewski, 2020). The historical storm surge of 1872 reached sea levels of more than 3 m in the Western Baltic Sea (e.g. Hofstede and Hamann, 2022), with an estimated return period of about 1,000 to 3,000 years, depending on the location and the statistics (MacPherson et al., 2023). This event resulted from a very high preconditioning and an exceptionally high storm surge, which could have been even higher (Andrée et al., 2023). Another event was recorded in 2005 for the Gulf of Riga with a maximum sea level of 2.75 m at Pärnu (Suursaar and Sooäär, 2007; Mäll et al., 2017). Historical events like these are often considered statistical outliers that do not seem to belong to the main population of extreme events (Hofstede and Hamann, 2022; Suursaar and Sooäär, 2007). However, their inclusion in the statistics is beneficial as they can significantly change the design sea level for coastal protection (MacPherson et al., 2023).

Storm surges are driven by winds and air pressure, the primary forces acting on the sea surface. However, the enclosed nature of the Baltic Sea limits the distance over which the momentum for storm surges can be deposited. Additionally, the northern Baltic Sea is partially covered by sea ice from winter to spring (e.g. Luomaranta et al., 2014). Sea ice acts as a lid, hindering the transfer of momentum from the wind to the water, reducing the ESLs by several decimetres (Zhang and Leppäranta, 1995). These factors, combined with short fetch lengths, generally result in lower return levels for the Gulf of Bothnia, except at its northern head, where the fetch length is maximal for southerly winds (Wolski et al., 2014; Lorenz and Gräwe, 2023a).

Among all the contributors to ESLs in the Baltic Sea, this study quantifies the contributions of the filling or preconditioning, seiches, and the storm surges to ESL events by performing a temporal decomposition. The second focus is quantifying different forcings' relative importance on the ESL events by performing numerical simulations. We quantify the role of the following forcings: wind, air pressure, North Atlantic sea level, baroclinicity, and sea ice.

2 Data and Methods

2.1 Observational gauge data

The observational tide gauge data are obtained from the European Marine Observation and Data Network (EMODnet, https://emodnet.ec.europa.eu, last access: 5 June 2021) and the Global Extreme Sea Level Analysis (GESLA Woodworth et al., 2016; Haigh et al., 2022). Both data sources provide quality-controlled sea level data at hourly frequency and high accuracy

(1 cm). We have selected 70 gauges (see Fig. 1 for their locations) to i) study the temporal decomposition of the observed ESL events and ii) validate the modelled ESL events to ensure that the temporal decomposition agrees with the observations.

Before any analysis, we selected the years 1961 to 2018 (the same time period covered by the model run, see next section) and subtracted the long-term linear trend of the mean sea level for each tide gauge. De-trending removes mean sea level rise and glacial isostatic adjustments (GIA Peltier, 2004) from the time series. Note that some gauges have records shorter than the considered time period and many contain temporal gaps (Lorenz and Gräwe, 2023a).

2.2 Numerical Simulations

We use the General Estuarine Transport Model (GETM, version 2.5 Burchard and Bolding, 2002) to simulate the sea level dynamics of the Baltic Sea. GETM has been used to model the hydrodynamics of several marginal seas and estuaries around the world. It has successfully demonstrated its ability to capture the complex hydrodynamics of the Baltic Sea (Gräwe et al., 2015), the mean sea level dynamics of the Baltic Sea (Gräwe et al., 2019), and its extreme sea levels (Lorenz and Gräwe, 2023a; Kiesel et al., 2023a). The model configuration is the same as in Lorenz and Gräwe (2023a) for their ensemble member *UERRA (baroclinic)*. The configuration uses a model chain starting in the Northwest Atlantic (5 NM resolution, bottom roughness $z_0 = 5$ mm) to generate boundary conditions for the North Sea and Baltic Sea domain (1 NM resolution, bottom roughness $z_0 = 1$ mm, Fig. 1), see e.g. Gräwe et al. (2015). Along the boundary of the Northwest Atlantic domain, air pressure-induced sea level changes (inverse barometric effect) are prescribed by the ERA5 reanalysis (Hersbach et al., 2020), which is also used as the atmospheric forcing for this setup. In this way, large pressure systems over the Atlantic are included in the model chain. The North Sea and Baltic Sea setup is forced by the *Uncertainties in Ensembles of Regional ReAnalyses* (UERRA Ridal et al., 2017), where the winds are increased by 7% to better represent the ESLs in the Western Baltic Sea (Lorenz and Gräwe, 2023a). The spatial resolution of the UERRA forcing is 11 km and the temporal resolution is hourly. Tides are not considered as they are negligible for the Baltic Sea. Static monthly mean density fields and sea ice cover are obtained from Gräwe et al. (2019). Wind stress reduction by sea ice is considered as in Gräwe et al. (2019). The advection scheme is the Superbee TVD scheme (Pietrzak, 1998). The simulation period is 1961 to 2018. We save sea level data in a time step of 20 minutes.

We exclude different forcing components in distinguished model simulations to investigate their effects on the sea level, see Tab. 1, i.e. seven simulations of the period 1961 to 2018. The respective difference to the *Full* simulation, where all components are included (the same model simulation as used by Lorenz and Gräwe (2023a)), is then attributed to be the effect of the excluded forcing. A detailed description of the decomposition approach is presented in the following sections.

2.3 Decomposition Approach

2.3.1 Temporal decomposition

We first split the time series of sea level elevation into three contributions: the surge η_{surge}, the filling state of the Baltic Sea η_{fill}, and the seiches η_{seiche}:

$$\eta_{\text{ESL}} = \eta_{\text{surge}} + \eta_{\text{fill}} + \eta_{\text{seiche}}. \tag{1}$$
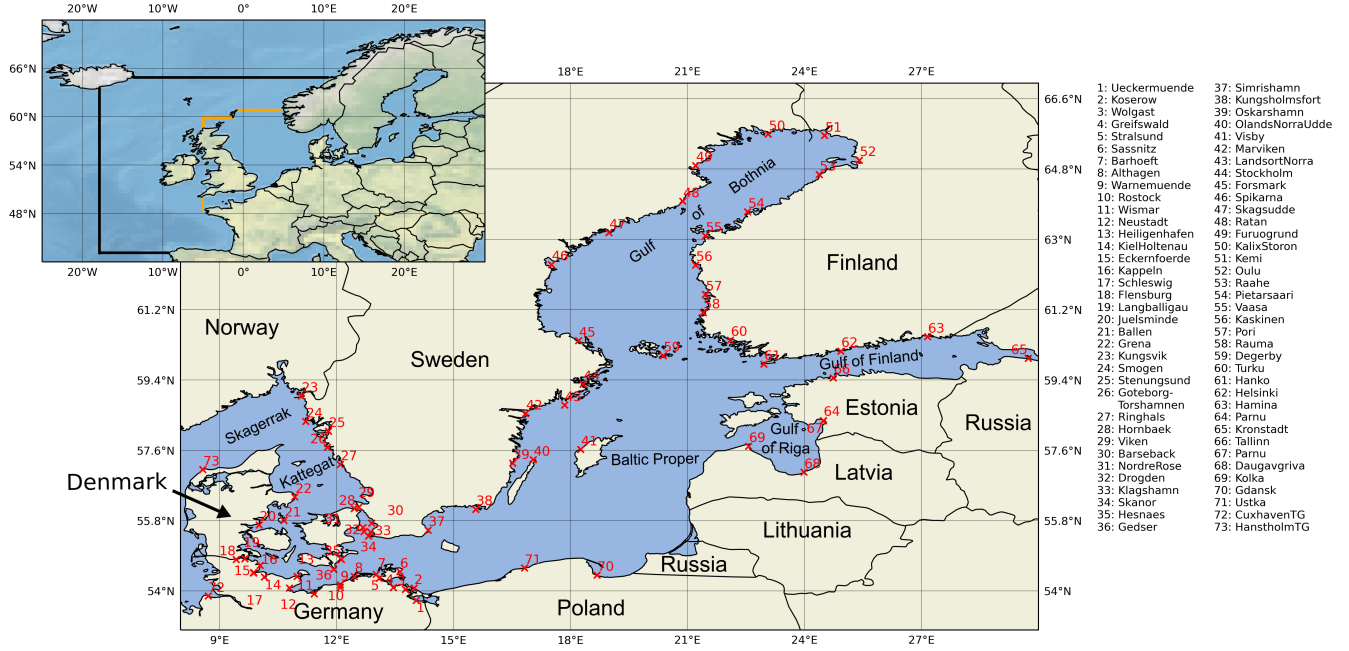
Figure 1. Model domain and station locations (red crosses and numbers) used for the temporal decomposition and model validation. The black line indicates the boundary of the coarse Northwest Atlantic Ocean domain. The orange lines mark the boundaries of the one nautical mile domain of the North Sea & Baltic Sea.

Table 1. Overview of the different simulations performed in this study.

Name	Description
Full	Simulation where all components are included.
NoWind	Simulation where the wind speed is set to zero, $u_{10} = v_{10} = 0$.
NoPresgrad	Simulation where the atmospheric pressure is constant, $P = 1000\,\text{hPa}$.
NoAtl	Simulation where the sea surface elevation, i.e. the sea level at the open boundary, is set to zero.
TSClim	Simulation where the inter-annual variability of temperature and salinity are excluded by using a climatology of temperature and salinity fields.
IceClim	Simulation where the inter-annual variability of sea ice cover is excluded by using a climatology of sea ice cover.
NoIce	Simulation where the sea ice cover is not considered.

125 ESL events η_{ESL} are identified by applying a peak-over-threshold method. The threshold is determined by the 99.7th percentile of the time series, and we only consider events that are separated by more than 48 hours (Arns et al., 2013). The filling state η_{fill} is computed by applying a Butterworth low-pass filter with a cut-off frequency of 7 days, corresponding to the weekly timescale described by Soomere and Pindsoo (2016) and Pindsoo and Soomere (2020). This time scale includes both the average filling state of the whole Baltic Sea and local filling due to persistent winds such as storm systems. To extract the seiche contribution

130 η_{seiche} from the time series, we consider a time window of ± 7 days around the peak sea level and force a fit of fixed frequency oscillations f_i:

$$\eta_{\mathrm{seiche}} = \sum_i a_i \sin\left(\omega_i t - \phi_i\right), \tag{2}$$

where i denotes the index of the frequencies considered, a_i and ϕ_i are the fitted amplitude and phase lag of the seiche, respectively, and $\omega_i = 2\pi f$. For the Baltic Sea, the dominant frequencies f_i we consider are: $(13\,\mathrm{h})^{-1}, (23\,\mathrm{h})^{-1}, (25\,\mathrm{h})^{-1}, (27\,\mathrm{h})^{-1}, (29\,\mathrm{h})^{-1},$

135 $(41\,\mathrm{h})^{-1}$ (Wübber and Krauss, 1979; Zakharchuk et al., 2021). Note that even more frequencies could have been added, but the amplitudes of these frequencies are much smaller. In addition, since we are considering $\mathcal{O}(100)$ events per station, the uncertainty estimates based on these statistical samples will be larger than the missing frequency contributions. Therefore, the errors introduced by neglecting these additional frequencies are expected to be negligible for this study. The surge component is then computed with:

140 $$\eta_{\mathrm{surge}} = \eta_{\mathrm{ESL}} - \eta_{\mathrm{fill}} - \eta_{\mathrm{seiche}}. \tag{3}$$

This temporal decomposition is done for both the observed and modelled ESLs.

2.3.2 Decomposition into forcing contributions

In addition to the temporal decomposition, we assume that each contributor in (1) can be linearly decomposed as the sum of the sea levels driven by the forcing components, namely wind η_{wind}, air pressure η_{pres}, sea level of the Atlantic η_{Atl}, inter-annual

145 variability of the baroclinic velocities due to seawater density gradients η_{barocl}, sea ice η_{ice}, and the inter-annual variability of the sea ice cover $\eta_{\mathrm{icevariability}}$:

$$\eta_j = \eta_{\mathrm{j,wind}} + \eta_{\mathrm{j,pres}} + \eta_{\mathrm{j,Atl}} + \eta_{\mathrm{j,barocl}} + \eta_{\mathrm{j,ice}} + \eta_{\mathrm{j,icevariability}} + \eta_{\mathrm{j,res}}, \tag{4}$$

where j denotes *surge*, *fill*, and *seiche*, respectively. Since there are interactions between the sea levels driven by the different contributors, we have included the residual term η_{res}, which essentially represents the difference between η_j and the sum of

150 the sea level contributions on the right-hand side, excluding the residual term itself. To extract the effect of each forcing, we subtract the respective simulation where we have excluded one component from the simulation *Full* (compare Tab. 1). For example, the time series of the sea level evolution due to wind forcing is computed by:

$$\eta_{\mathrm{wind}} = \eta_{\mathrm{Full}} - \eta_{\mathrm{NoWind}}. \tag{5}$$

The other forcing contributions are computed accordingly.

2.4 Work flow of the time series analysis

As a first step, the long-term changes in the mean sea level are removed from the time series by de-trending by subtracting the linear trend of the entire time series; see Fig. 2a. The filling time series η_{fill} is then computed by applying the Butterworth low-pass filter with a cut-off frequency of 7 days, as mentioned previously. ESL events are identified in the de-trended time series by applying a peak-over-threshold method. The threshold is determined by the 99.7th percentile of the time series, and we only consider events that are separated by more than 48 hours (Arns et al., 2013). For the modelled time series spanning 58 years from 1961 to 2018, approximately 80 to 250 events are identified for each station. The station locations are shown in Fig. 1. The number of events in the observed time series may differ due to the varying length of the time series and data gaps. Note that the search for ESL events is only performed for the *Full* simulation.

We consider a time slice of plus-minus 7 days for each event around the peak sea level. From the resulting shorter time series, the respective filling is first subtracted. Then, the seiches are forced-fitted with eq. (2), followed by the computation of the surge component with eq. 3. An exemplary temporal decomposition of the observed Warnemuende time series (Fig. 1, station 9) is shown in Fig. 2b. For each temporal component, we record the respective sea level occurring at the time of the peak sea level (dashed line in Fig. 2b). This results in a sample of sea levels for the total peak level and its respective components from the temporal decomposition. In addition, the maximum filling and maximum seiche level values within a 48-hour window, i.e. $\pm 24\,\text{h}$ around the ESL peak, are stored to assess the potential ESL if all three components were to reach their peaks simultaneously.

To study the relative importance of each component, the components are normalised to the peak level for each event and stored in a histogram with a bin size of 0.01, ranging from -0.5 to 1.2. The normalisation allows us to utilize all events to make general statement of the mean composition of ESLs. Each histogram is used to fit a Gaussian distribution to extract the mean and standard deviation; see Fig. 2d. For this station, the mean temporal contributions are: 60.5% surge, 26.5% filling, and 12.9% seiche (sum: 99.9%). Similar to the methodology described, each temporal component of *filling*, *seiche*, and *surge* is decomposed into the contributions of the different forcings, as shown in Fig. 2c,e for the *surge* component as an example. Since the sea ice component can only lower the sea level, the Gaussian fit approach is unsuitable, due to its non-Gaussian distribution. Therefore, for the sea ice component, the mean and standard deviation are computed directly from the sea levels and then normalised. For the station Warnemuende, the mean forcing contributions are: 84.5% wind, 8.0% air pressure gradients, 2.9% Atlantic sea level, 0.2% baroclinicity of seawater, -0.5% sea ice, 0.2% sea ice variability, and 1.8% residual (sum 97.1%). Due to the uncertainty in the fits, we cannot expect the sum of all forcings to add to 100.0%.

Note that the distribution of ESLs generally follows a tail-end statistical distribution such as the Generalised Extreme Value or Generalised Pareto distribution. The filling component follows a classical asymmetric quasi-Gaussian distribution (Soomere et al., 2015). However, as we generate samples of relative contributions to normalised peak sea levels, these samples are expected to follow a Gaussian distribution (except for the sea ice component).
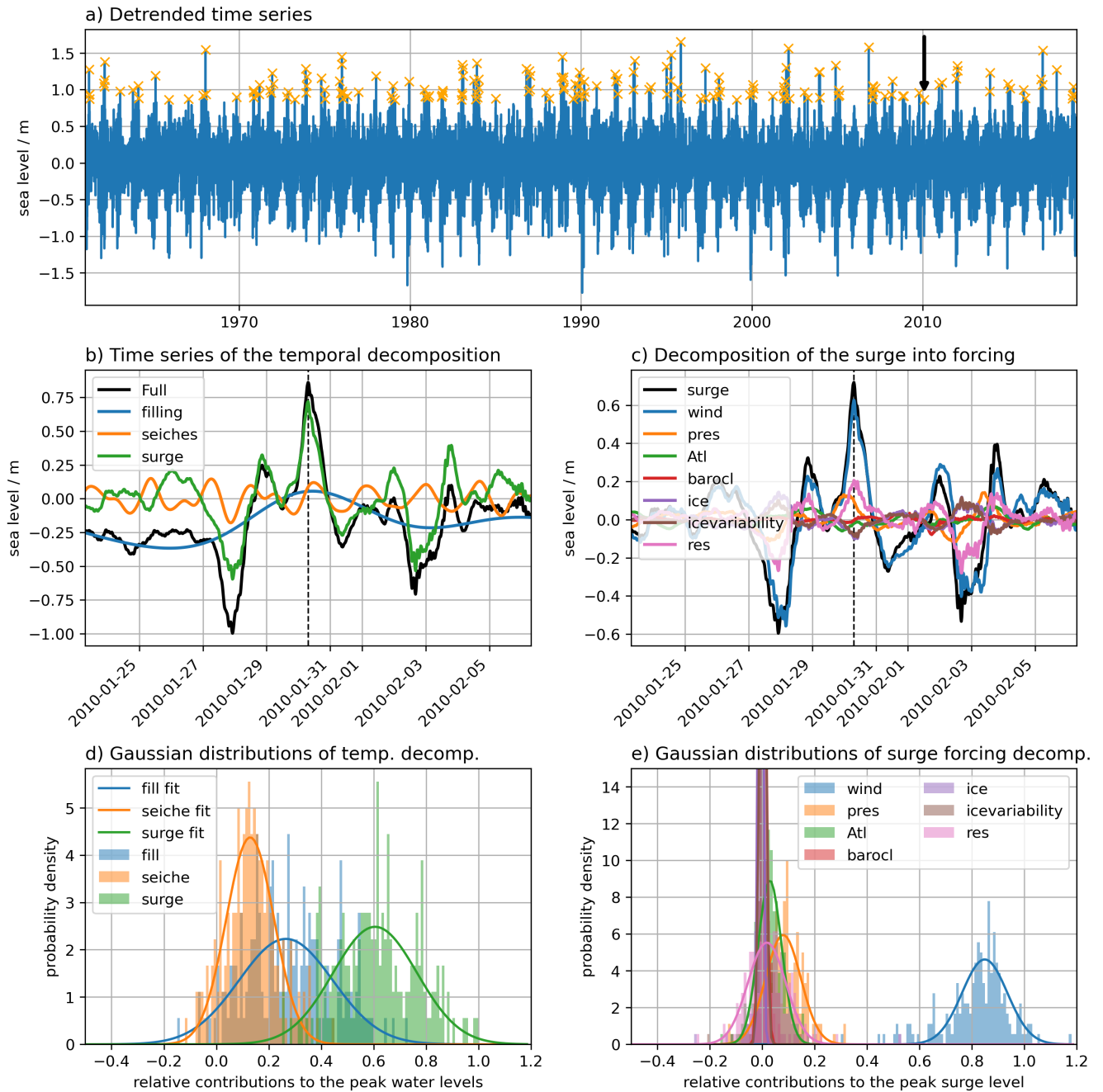
Figure 2. Exemplary results of the workflow for the decomposition of ESL events: a) The de-trended time series of the station *Warnemuende*. The orange crosses indicate all considered ESL events. The black arrow denotes the exemplary event that is decomposed in panels b) and c). b) Temporal decomposition into *filling*, *seiche*, and *surge* components around the peak sea level of the event. c) Decomposition of the *surge* component into the different forcings. The dashed black line in b) and c) marks the time of the peak sea level. d) The histograms and fitted Gaussian distributions of the temporal decomposition using all the events marked in a). e) Similar to d) but for the decomposition into forcing contributions for the *surge* component.

3 Results

3.1 Temporal decomposition

The temporal decomposition of the observed ESLs indicates that in the Western Baltic Sea, the surge component accounts for more than 60% of the ESL events for all stations (Fig. 3a,b). Following the surge component, the seiche and filling components contribute almost equally. For the westernmost stations, the seiche contribution exceeds that of the filling. In contrast, stations located along the eastern German coast show a greater contribution of the filling component, indicating that these stations are closer to the seiches' pivot point(s) and, therefore experience smaller seiche amplitudes. Note that the seiche periods of 23 to 29 h are in the range of the duration of the surge events in this region of the Baltic Sea (Kiesel et al., 2023b). Along the southwestern coast of the Baltic Sea towards Sweden, the largest contribution shifts from the surge to the filling component. The filling component contributes 50 to 75% of the total ESL along the coasts of the Baltic Proper and the Gulf of Bothnia (Fig. 3a,c). For most of the Swedish coast, the remaining contribution to the ESL is the surge component, with almost negligible seiches (Fig. 3a,d). A similar pattern is found on the Finnish coast in the Gulf of Bothnia. In the Gulf of Finland, the surge is the second largest contributor, followed by the seiche component, with the filling component remaining the largest contributor. The surge component becomes more significant as a tide gauge is located further east in the Gulf of Finland, due to the increased fetch length over which the wind can transfer momentum to the sea. In the Gulf of Riga, the seiche component is again negligible and the contribution of surges to the ESLs is nearly as significant as that of the filling. For the Polish stations, Gdansk and Ustka, the decomposition is similar to that of the Gulf of Riga, with almost negligible seiches.

Comparison of the gauge data decomposition with the numerical model results, Fig. 3b-d, shows that the model statistics agree with the observed statistics. Differences are found for gauges that are located within coastal lagoons or estuaries, such as Ueckermuende, Althagen, Barhoeft, Kappeln, Schleswig, and Gdansk, since the hydrodynamics are not resolved at the 1 N.M. resolution of the model, as discussed by Lorenz and Gräwe (2023a). Note that even a 200 m resolution is insufficient to reproduce the hydrodynamics in these areas, resulting in the model overestimating ESLs in these regions (Kiesel et al., 2023b).

Although located outside the semi-enclosed Baltic Sea, stations in the Kattegat and Skagerrak (stations 20-28) and in the North Sea (station 73) still exhibit large filling contributions of 40-50%. This shows that, at least for ESL events, low-frequency waves such as the filling contribute to the slow sea level variability. This makes sense as the mean filling of the Baltic Sea is controlled by the water exchange with the North Sea, which requires long periods of elevated sea level in front of the Danish Straits. Since tides are excluded in the simulations, the low-frequency variability cannot be a superposition effect such as the spring-neap cycle, further indicating that low-frequency waves also contribute significantly to ESLs in the more open eastern North Sea. As a contrast to the Baltic Sea stations, we included one station in the North Sea, Cuxhaven (72). The model deviates from the observations for this station in the southeastern North Sea because tides are not included in the model. Nevertheless, the filling contribution of about 25% to the ESLs is a noteworthy result, indicating that persistent westerlies can elevate the mean sea level for a period of at least one week and longer in this region.
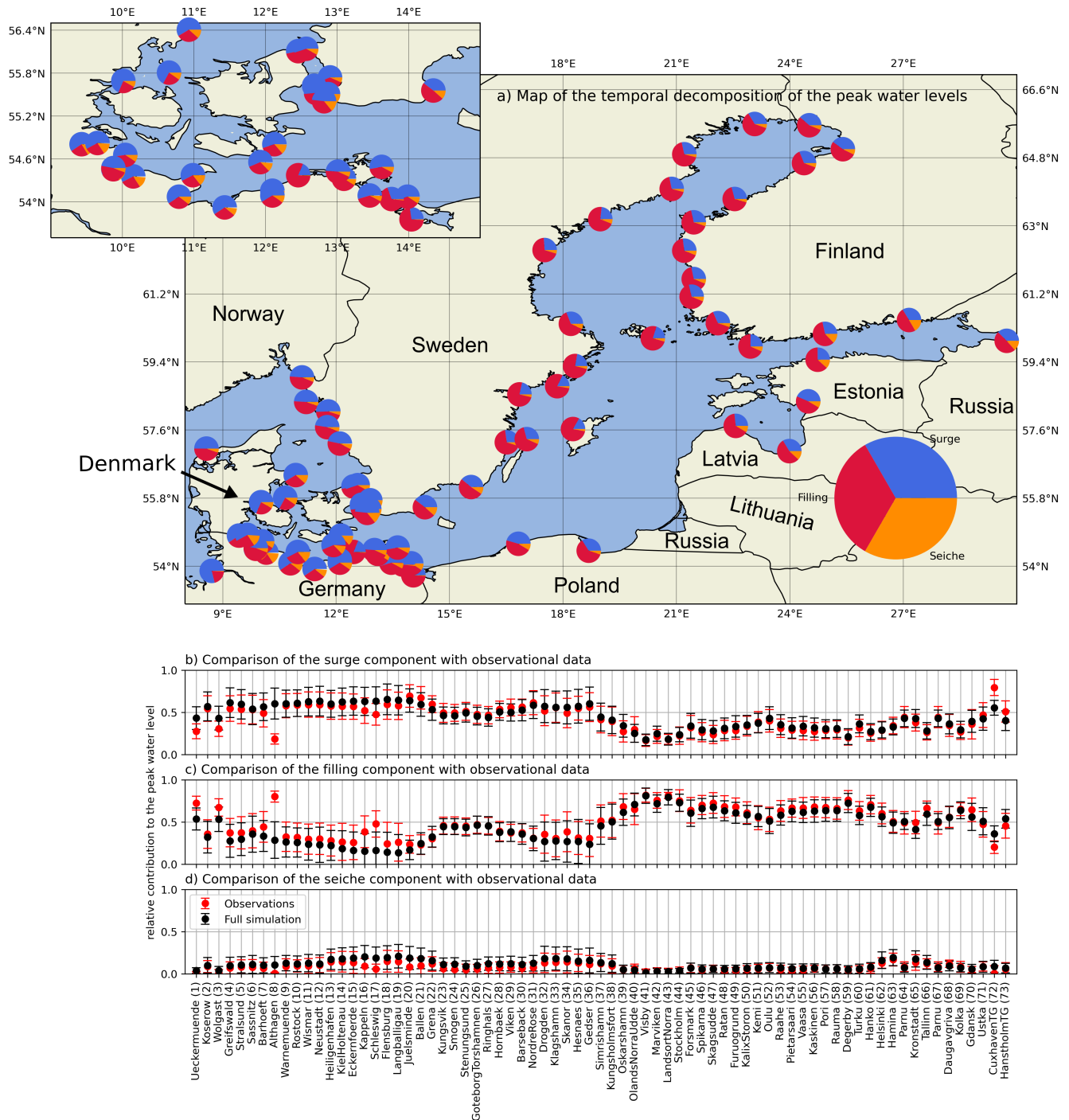
Figure 3. Temporal decomposition of the peak sea levels: a) Map of the temporal decomposition of the ESL events in the observations for each station. b) Comparison of the modelled *surge* component with the *surge* component from the observed sea level data. The mean (dots) and standard deviation (caps) are obtained from the Gaussian distribution fits (except for sea ice simulations, see Section Workflow), compare Fig. 2d. c) As b) but for the *filling* component. d) as b) but for the *seiche* component.

3.1.1 Correlations between the components

A correlation analysis (Pearson's correlation coefficient) of the three temporal components (Fig. 4a-c) reveals that the filling and the surge components are negatively correlated for the western and central Baltic Sea (Fig. 4a). The filling and the seiche components show only a weak negative correlation (Fig. 4b). The seiche and surge components are positively correlated for the central and eastern Baltic Sea (Fig. 4c).

The negative correlation between surge and filling is surprising at first sight, as it is known that most ESLs in the Baltic Sea are a coincidence of both contributions. At second glance, it does not contradict the fact that most ESLs are a combination of high filling states and storm surges which would intuitively indicate a positive correlation. The negative correlation between the relative filling and surge components is partly an artefact of the decomposition method since we do not correlate the whole time series, but only the extracted statistical samples which we used for the Gaussian distribution fits. Since the peak sea level of each event is fixed, a particularly high surge (right side of the surge's Gaussian distribution) must naturally coincide with a lower filling state relative to the mean of the Gaussian distribution (left side of the filling's Gaussian distribution), which emphasizes a negative correlation. Otherwise, the average relative ESL would be higher than 100% and thus the fitted Gaussian distributions would be wrong. The same applies to a low surge and a high filling state. Therefore, these two components must be negatively correlated in this decomposition approach of the mean ESL. For the Warnemuende station this negative correlation is clearly visible, both for the modelled and the observed ESL events (Fig. 5, here with non-normalised sea levels). Of course, events where both the filling and the surge components are very high relative to their mean are also possible and observed (Groll et al., 2024). For example, some of the highest peaks at Warnemuende, exceeding 1.5 m (Fig. 5b, events numbers 33, 52, 73, 110), are formed by the combination of very high surge and high filling components. However, the probability of occurrence of extremely high filling and surge combined ESL events is low. Nonetheless, these events are often among the most devastating ones and can lead to dangerous inundations in the coastal regions, e.g. the historic 1872 surge (Hofstede and Hamann, 2022).

The positive correlation between the seiche and the surge can be explained by the initialisation of the seiche by preceding weather systems before the actual surge occurs, i.e. seiches are excited by a previous surge. The stronger the subsequent system, the higher the seiches initialised by the previous system are likely to be. It is also likely that the frequency of the seiches is comparable to the duration of the surges, so the forced fit may overestimate the height of the seiches during the ESL event. Areas where the correlation is low and not significant indicate that the phase of the seiche during the surge's peak is random.

The negative correlation between filling and seiches shows smaller coefficients than between filling and surge components, indicating that seiches tend to be small when filling is high and vice versa. Since there is a positive correlation between surges and seiches, and a negative correlation between filling and surges in the same areas, it makes sense that seiches should generally be negatively correlated with filling as well.

3.1.2 Potential increases of maximum sea levels by time shifting the components

Since the low-frequency waves of the filling component and the high-frequency contributions from seiches and surges operate on different time scales, the timing of their peaks should be independent of the filling levels, essentially making them random.
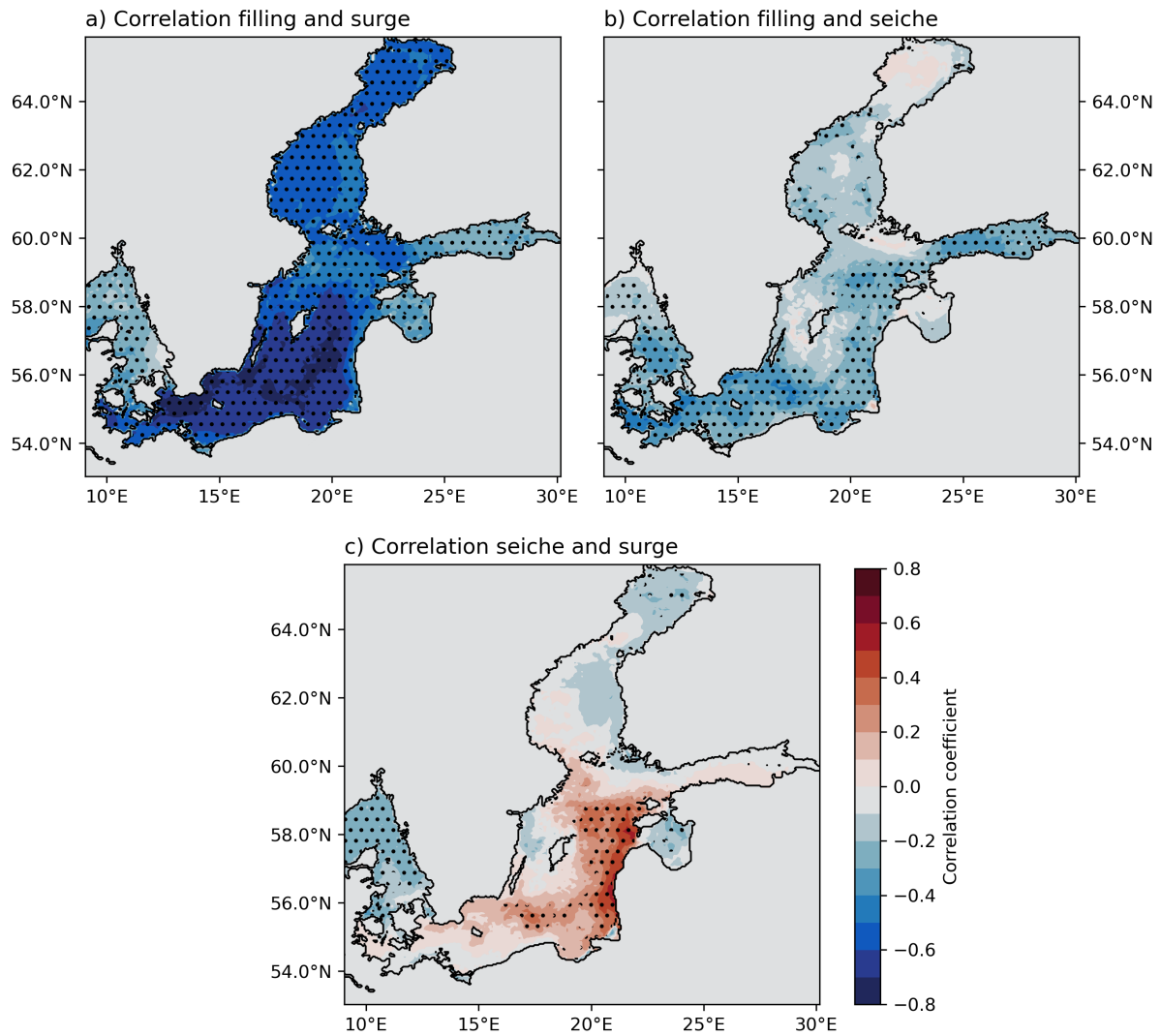
Figure 4. Correlation maps for the three temporal components: a) Correlation coefficient for *surge* and *filling* components. b) Correlation coefficient for *filling* and *seiche* components. c) Correlation coefficient for *seiche* and *surge* components. The hashed areas indicate where the p-value is below 0.05.
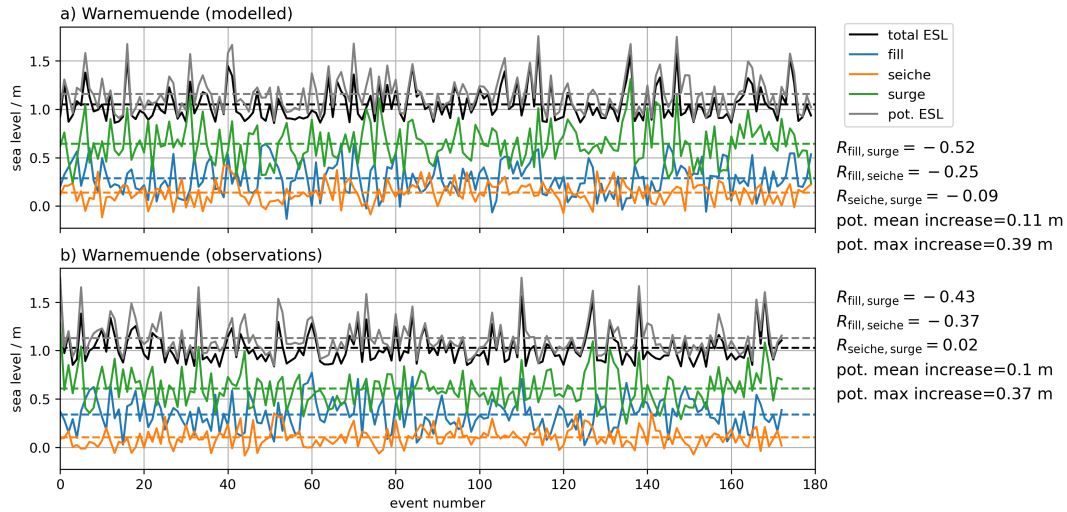
Figure 5. Illustration of the temporal decomposition and the correlation between the components for the station Warnemuende. a) The three components *filling*, *surge* and *seiche* for the modelled ESL event. b) As a) but using the observed ESL events. In grey, the maximum ESL heights are shown, e.g. the potential sea level if the surge peak, the seiche peak, and the maximum filling (all $\pm 24\,\mathrm{h}$ around surge peak) co-occurred.

Therefore, we assess the potential increase in peak sea levels under a worst-case scenario, where the peaks of all three components align. Specifically, we examine the maximum filling levels and seiche heights within a 48-hour window surrounding the ESL peaks. For the Warnemuende station, the mean and maximum potential increases due to these compounding components are $11\,(10)$ cm and $39\,(37)$ cm respectively, where the values in the brackets are from the observations (grey in Fig. 5). A more detailed examination of these potential increases shows that the filling component has less potential to increase the ESLs than the seiche component (Fig. 6a-d). On average, the filling could have increased the ESLs by only a few centimetres (Fig. 6a), whereas the maximum increase could have been in the range of 10-20 centimetres (Fig. 6b). If the seiche peaks were aligned with the surge peaks, the mean increase could reach 10 cm (Fig. 6c) and the maximum increase of up to 30-40 cm (Fig. 6d). The largest mean increases are found in the western Baltic Sea and at the head of the Gulf of Finland with values between 10-15 cm (Fig. 6e). The largest maximum increases are also found in these regions with values reaching up to 50 cm (Fig. 6f). The large potential increases in the northern Baltic Sea most likely correspond to the effect of seiches introduced by preceding storms, i.e. the clustering of passing storm systems as described by Rantanen et al. (2024). The potential increases by seiches are small in the central Baltic Sea, where a positive correlation between the surge and the seiches is found (Fig. 4c).

3.2 Decomposition into forcing components

As expected, the surge component is almost entirely explained by the winds. Throughout the Baltic Sea, winds account for 80% and more of the surge heights (Fig. 7). The remainder is mainly explained by atmospheric pressure. Winds continue

13
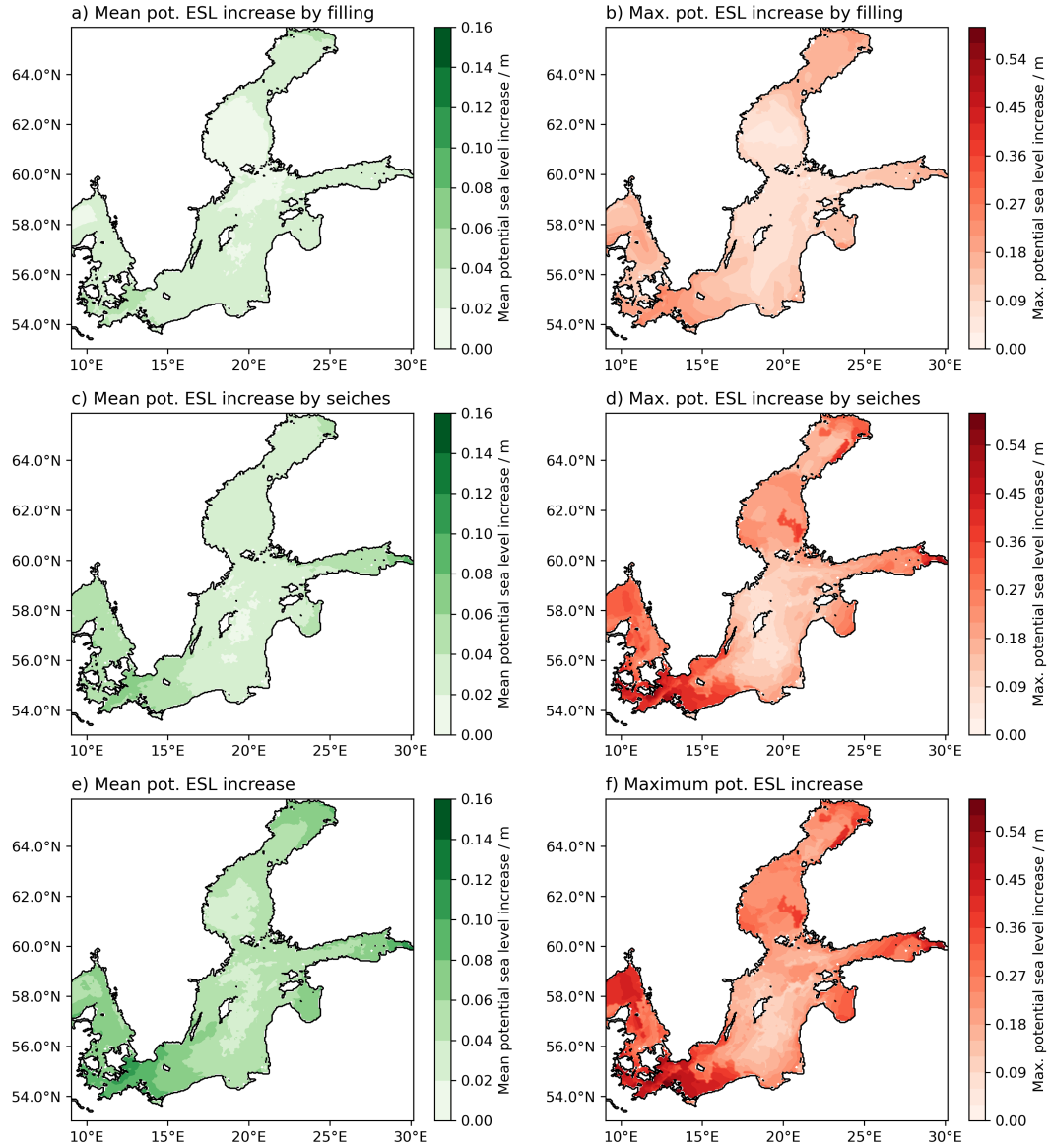
Figure 6. Potential increases of the ESL event if the three temporal components were compounding, e.g. their maxima occurred simultaneously: a) Mean potential increase from the filling component (difference maximum filling around the ESL peak (±24 h) to the actual filling at the ESL event). b) Maximum increase of the filling component. c) As a) but for the seiche component. d) As b) but for the seiche component. e) Potential mean sea level increase if the surge peak, the seiche peak, and the maximum filling occurred at the same time (sum of a) and c)). f) As e) but for the maximum ESL increase within all ESL events in the respective grid cell (sum of b) and d)).

being the most important surge forcing for the Kattegat, north of the Danish Straits and outside the Baltic Sea basin. However, the Atlantic sea level component can contribute up to 30% of the surge levels for this region. This indicates that some of the surges in this region originate outside the model domain. Their fetch lengths exceed the distance from the Kattegat/Skagerrak to the open boundary. Therefore, the origin of these surges is introduced by the boundary conditions of the Northwest Atlantic through the inverse barometric effect. The winds within the model domain then amplify these surges. The effect of sea ice is limited to the Gulf of Bothnia and the head of the Gulf of Finland, where the surge height can be reduced by 10% on average and even more for individual events, which is in the order of the expected magnitude (Zhang and Leppäranta, 1995).

Similarly, winds account for the seiche component almost everywhere, with minor contributions from atmospheric pressure in the Baltic Sea (Fig. 8). The Atlantic component also plays a role for Kattegat near the Danish Straits. Generally, the fitted seiche periods are based on the seiche frequencies in the Baltic Sea basin. Therefore, the chosen seiche frequencies likely do not correspond to the actual seiches for this region. This discrepancy may explain why the seiche component in the Kattegat and Skagerrak is the smallest contributor to the ESLs. Furthermore, sea ice has a minor influence on the seiches in the Gulf of Bothnia.

The filling component is also mainly determined by the wind forcing (Fig. 9), with contributions ranging from 50% in the Kattegat and Skagerrak to more than 80% in the Western Baltic. For the Western Baltic Sea, atmospheric pressure is the second largest contributor to the filling component. The other forcings contribute a few percent to the mean filling for the rest of the Baltic Sea basin. In contrast to the surge and the seiche components, the residual term shows values of up to 20% within the Baltic Sea. The wind and Atlantic sea level forcings explain most of the filling for the Skagerrak and Kattegat. However, the residual term shows values up to 40% across these regions. These large residuals indicate that the assumed linearity of the decomposition into forcings does not hold well for the filling component, likely due to temporal shifts of low-frequency waves.

The results of the forcing decomposition show that the inter-annual variability of sea ice has a negligible effect on ESLs due to its minimal contribution to any of the three temporal components: surge, seiche or filling (Figs. 7-9). The inter-annual variability of the baroclinicity of seawater has no effect on the high-frequency surge and seiche components (Figs. 7- 8) and only a minimal effect on the filling component. The Atlantic sea level mainly affects the surge component for the Kattegat and Skagerrak, while its contribution to the filling component is limited to a few percent. As expected, the wind and air pressure forcing are the main forcings for all three components, with the wind being the most important.

4 Discussion

4.1 Components

#### 4.1.1 Importance of the components and forcings

Our results show two distinct temporal compositions of the ESLs: In the Western Baltic Sea, the primary component is the surge, which acts upon the local filling state and is modulated by the seiche component. In contrast, filling is the primary driver in the rest of the Baltic Sea basin, with relatively smaller surges acting on top. Again, the seiches modulate the peak sea level.

15
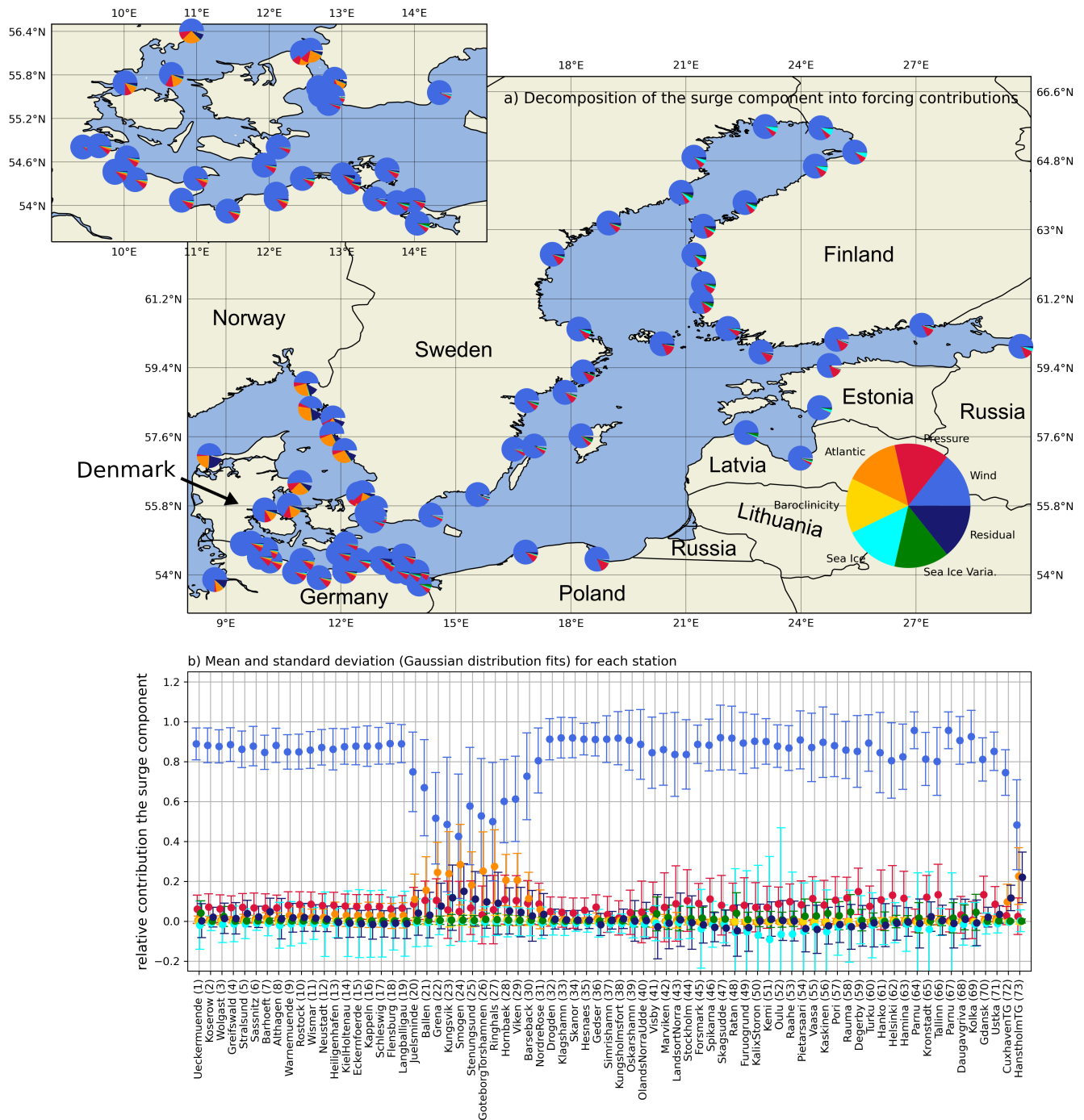
Figure 7. Decomposition of the *surge* component into forcing contributions: a) Pie charts of the relative forcing contribution for each station scattered over the Baltic Sea. b) Relative contributions regarding mean and standard deviation (based on Gaussian fits) for each station. Note that the pie chart depiction only considers the absolute values and not the sign.

16
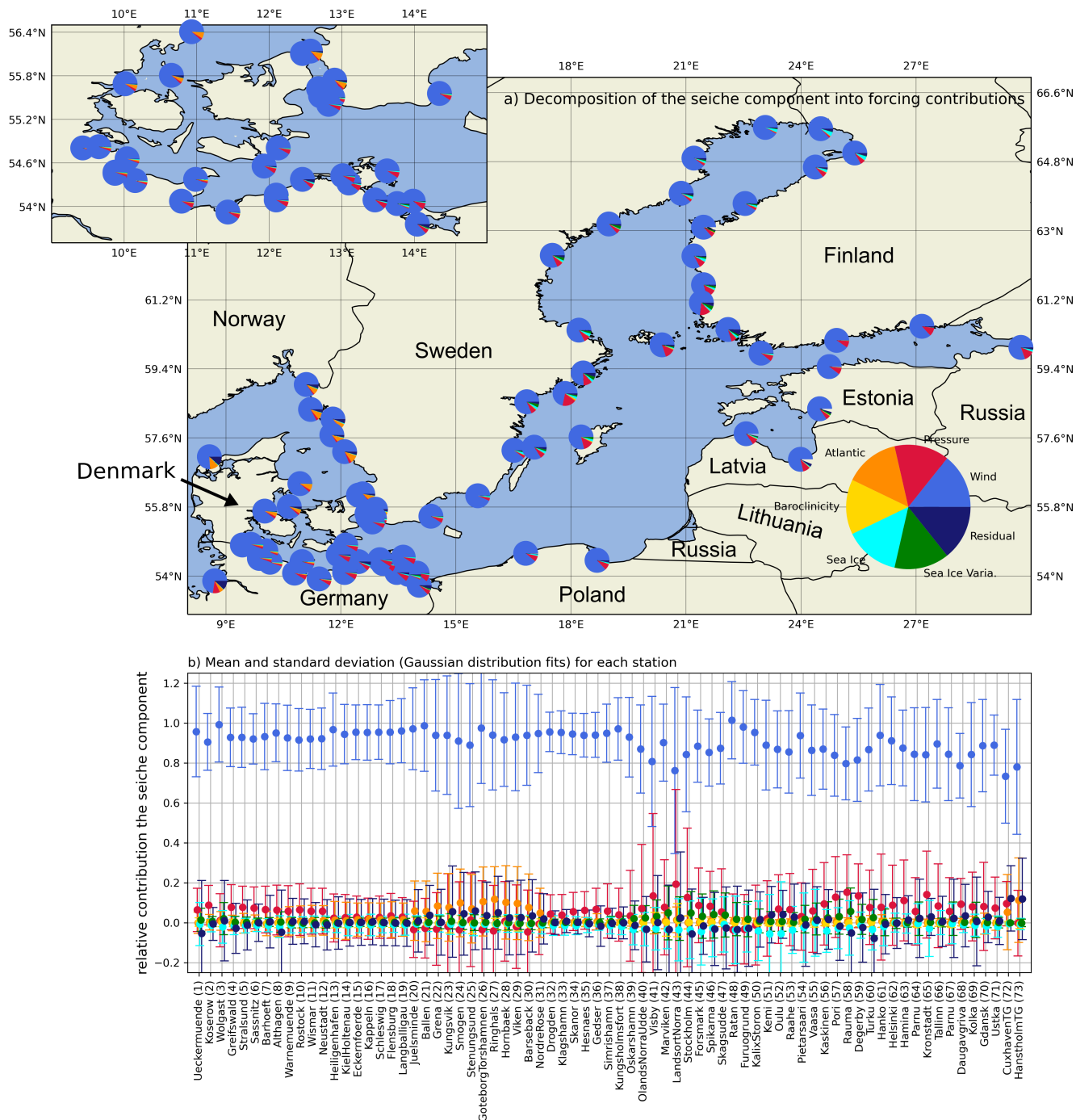
Figure 8. Decomposition of the *seiche* component into forcing contributions: a) Pie charts of the relative forcing contribution for each station scattered around the Baltic Sea. b) Relative contributions regarding mean and standard deviation (based on Gaussian fits) for each station. Note that the pie chart depiction only considers the absolute values and not the sign.
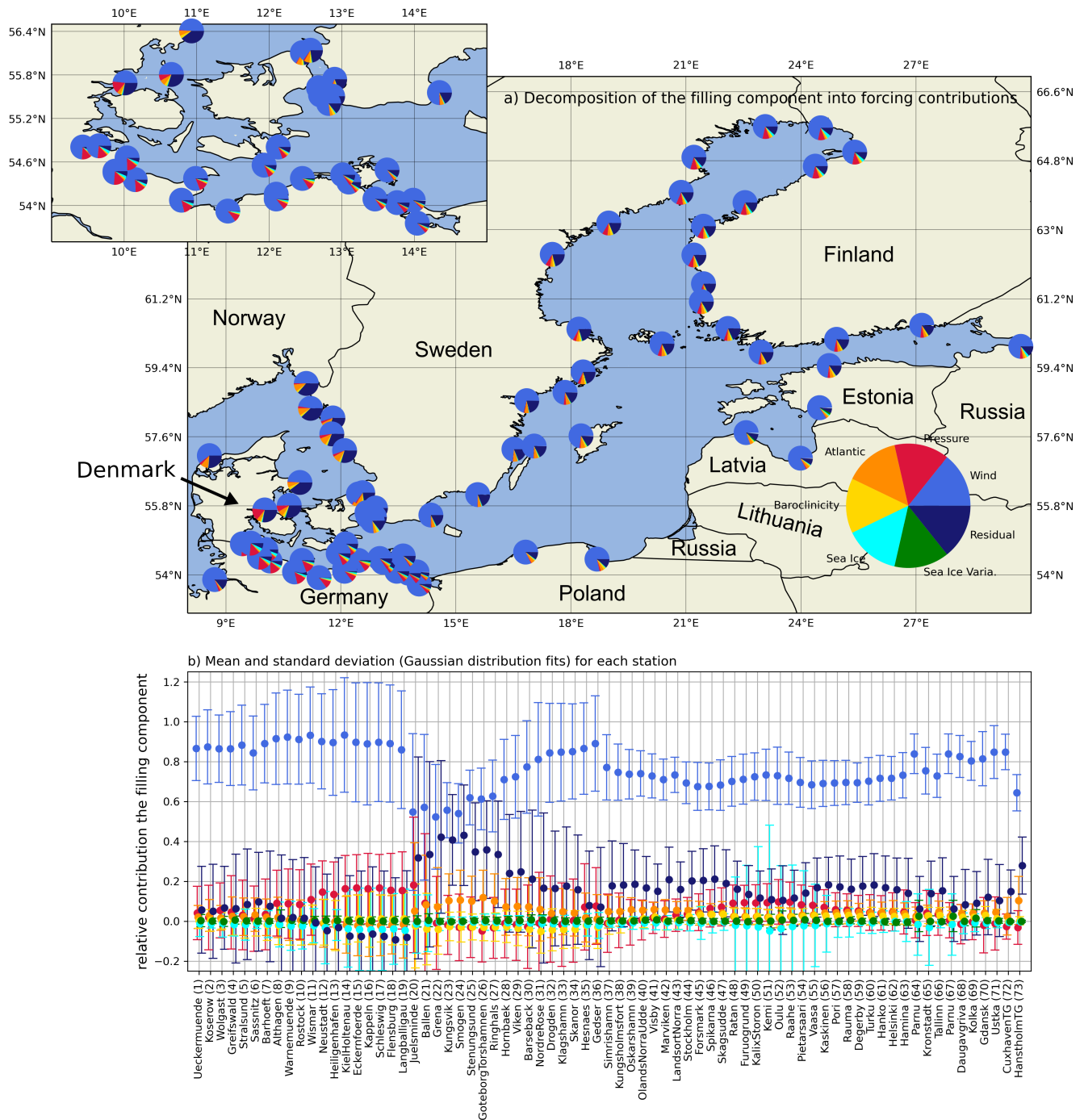
Figure 9. Decomposition of the *filling* component into forcing contributions: a) Pie charts of the relative forcing contribution for each station scattered around the Baltic Sea. b) Relative contributions regarding mean and standard deviation (based on Gaussian fits) for each station. Note that the pie chart depiction only considers the absolute values and not the sign.

For the Kattegat and Skagerrak outside the semi-enclosed basin, the contributions of filling and surge are almost equal, with the seiche being the least contributing component. Different primary contributors can lead to variations in the characteristics of ESLs, potentially causing differences in their dynamics, persistence, and probability of occurrence at specific locations.

This distribution of two distinct contributors to ESLs corresponds to the dominant wind climatology in the Baltic Sea region. Westerly winds generate high filling (Gräwe et al., 2019) and often cause storm surges on the west-facing coasts of the Baltic Sea. There, the filling is the main contributor, and surges also play a significant role. The east-facing coasts of the Baltic Sea are sheltered from these prevailing winds, so that the filling component is the most influential factor there, with the exception of the Western Baltic Sea. While strong winds from the north and east are less frequent (Soomere and Keevallik, 2001), these winds cause surges along the coasts of Germany, Denmark and Sweden.

Although the importance of the filling component has been recognised in the literature before (e.g. Soomere and Pindsoo, 2016; Pindsoo and Soomere, 2020), this study provides quantitative figures that underline its significance. For the Western Baltic Sea, the mean contribution of filling is less than the contribution of the surge, which is consistent with the recent results of Groll et al. (2024), who studied the contribution of surge and filling in the Western Baltic Sea. This is partly because water can flow into the Kattegat, Skagerrak and the North Sea on the time scale of the filling, which is about a week. Nevertheless, it is a fact that both filling and surge have compounded for the highest ESL events that caused severe historical inundation and damage, e.g. 1872 (Hofstede and Hamann, 2022) or 2005 (Suursaar and Sooäär, 2007; Mäll et al., 2017).

We have demonstrated that temporal shifts towards simultaneous alignment of the maximum sea levels of the three temporal components can increase the ESLs by several decimetres within the respective event. It has to be noted that the forced-fitting approach can lead to a positive bias of potential increases, especially if the surge duration is similar to one or more of the seiche periods. Therefore, the maximum potential increase due to the seiches (Fig. 6d) and hence the maximum total increases (Fig. 6f) are most likely overestimated. Nevertheless, the potential average increase due to temporal shifts in the seiche and filling is in the order of 10-20 cm. These values represent the theoretical maxima of ESLs in the respective regions for the specific events.

Our analysis of the forcing contribution clearly shows that wind and air pressure are by far the most important contributors to the ESLs in the Baltic Sea region.

Sea ice is known to reduce the local momentum transfer to the water and therefore reduce storm surges (see Zhang and Leppäranta, 1995, for the Baltic Sea). For the northern Baltic Sea, sea ice is present every winter during the storm season, which we have included in our simulations. Our model simulations suggest that sea ice reduces the surge component by 10% on average, translating into sea level changes in the range of decimetres shown by Zhang and Leppäranta (1995). In regions where sea ice is present in winter, the filling component is the main contributor to ESLs, which is almost unaffected by sea ice as filling is a basin-wide process. However, with decreasing levels of sea ice due to climate change (e.g. Meier et al., 2022a, b, and references therein), the contribution of storm surge to ESLs is likely to increase in the future in regions that are currently covered by annual sea ice. The same argument can be made for the inter-annual variability of sea ice. Our results show that this contribution to the ESLs is currently very small (Figs. 7-9). However, in a warming climate, the contribution of inter-annual variability of sea ice may increase.

335 The inter-annual effects of baroclinic density fields to ESLs are found to be negligible, indicating that baroclinic contributions to water transports are not important for ESL events in the Baltic Sea.

4.1.2 Excluded components and forcings

Many coastal regions of the world have tidal regimes that allow ESLs to occur only during high tide and also interact with storm surges (Arns et al., 2020). The tides are generally very small ($< 10\,\text{cm}$) and confined to the Western Baltic Sea (e.g.

340 Gräwe and Burchard, 2012). Therefore, we expect tide-surge interactions to be small (Arns et al., 2020). Their mean relative contribution to ESL events should be zero, as the occurrence of the surge should be uniformly distributed over the tidal cycle. Consequently, we have deliberately excluded the tidal component in our temporal decomposition. For tidal regions it can easily be added to the decomposition.

For the decomposition into forcings, we have also omitted the process of wave setup, e.g. momentum deposition due to

345 breaking surface wind waves, which can also contribute to ESLs (Longuet-Higgins and Stewart, 1964). In the eastern Baltic Sea in the Gulf of Finland, wave setup can contribute several decimetres to ESLs in some coastal segments, resulting in relative contributions of up to 50% (e.g. Soomere et al., 2013). It should be noted, however, that these estimates are subject to large uncertainties due to assumptions made about the relationship between the offshore wave heights and the wave setup itself. In the Western Baltic Sea, the effect of wave setup on ESLs is only a few centimetres (Su et al., 2024). However, the potential

350 contribution of wave setup can be substantial in specific locations, e.g. for exposed coasts of islands (Su et al., 2024) or coastal bays (Soomere et al., 2013). The challenge in accurately assessing the wave setup component lies in the need for high-resolution data on wind wave properties within the surf zone, which even state-of-the-art hydrodynamic models struggle to capture on large scale, such as the entire Baltic Sea. Running a wave model with such fine resolution at this scale is not feasible. As a result, distinguishing wave setup from the direct momentum transfer caused by wind remains a task for future research.

355 In general, the exclusion of wave setup should not affect our results much, as the model can reproduce the ESL statistics (Lorenz and Gräwe, 2023a) and the temporal decomposition of the observations (Fig. 3). Thus, the transfer of momentum from the atmosphere to the ocean via the transfer bulk formula is able to reproduce the ESLs. However, it should be noted that the wind speeds were increased by 7%, which was necessary to match the ESLs with the observations, especially in the Western Baltic Sea, see (Lorenz and Gräwe, 2023a) for a discussion of this issue. This increase may partly compensate for the

360 missing wave setup. Nevertheless, this would not diminish the relative importance of the wind forcing. It would only split the wind component into a direct sea level component, the generation of long surface waves, and an indirect sea level input via the breaking of surface wind waves within the surf zones.

Similar to wave setup, we have excluded meteotsunamis (Monserrat et al., 2006; Pattiaratchi and Wijeratne, 2015b). These are tsunami-like surface waves generated by the matching of the propagation speeds of a small atmospheric pressure jump and

365 the induced surface wave, e.g. a Proudman resonance (Proudman, 1929). The reasons for neglecting meteotsunamis are simple: First, the temporal and spatial resolution of the meteorological forcing is too coarse to resolve the propagating pressure system accurately enough to generate meteotsunamis in the numerical model. Second, the hourly resolution of the observational data used is also too coarse to resolve meteotsunamis that occur on faster time scales (minutes). Nevertheless, meteotsunamis could

occur during an ESL event (Pattiaratchi and Wijeratne, 2015a) and are a common phenomenon in the Baltic Sea (Pellikka et al., 2020, 2022) with high sea level contributions in the order of decimetres. Meteotsunamis could easily be included in the temporal decomposition using a high-pass filter.

We have also ignored the influence of river discharge since the coarse resolution of our model does not sufficiently resolve the estuaries and constrictions where river discharge increases sea level. However, compounding ESLs with very high river discharge can elevate the peak sea level (Talke et al., 2021) and have been observed in the southwestern Baltic Sea (Heinrich et al., 2023). We do not expect major changes in our results, as these effects are restricted to estuaries and we have studied ESLs at the open coast. Nevertheless, we acknowledge the importance of river discharge in estimating coastal flooding.

4.1.3 The residual term and non-linear interactions

In decomposing the different forcing components, a residual term has been added to the right hand side of eq. (4) to account for non-linear effects between the forcing contributions and unaccounted forcings. The residual term is not important for the seiche component. However, for individual events, the assumption of linear superposition may not hold since the standard deviation of the residual term is in the range of 10-20%. For the surge component, the decomposition into forcings works well. Both the mean residual and the standard deviation remain small, except for the Kattegat region. There, the residual term becomes notably large, indicating the presence of non-linear interactions. These interactions could affect both the sea level height and the timing, leading to temporal shifts. Similarly, the residual term for the filling component is non-zero throughout the Baltic Sea. Overall, the residual term is not negligible for any temporal component, clearly showing the interaction between the different forcings on the simulated sea levels. Nevertheless, our results quantify the relative importance of the different forcings to each other, which should be independent of the residual term.

The temporal decomposition performed in this study (1) does not allow the quantification of non-linear interactions between the different time scales. Although these non-linear interactions are included in the respective time series, the computation of the three components automatically attributes all non-linear interactions to the surge component, see eq. (3). However, the non-linear interactions between the temporal contributors are expected to be small in the Baltic Sea (Arns et al., 2020).

4.2 Consequences for ESL statistics

The results indicate that the three temporal components are correlated: there is a negative correlation between filling and surge, a weak negative correlation between filling and seiche, and a positive correlation between the surge and seiche. This suggests that the contributors are not independent, which has implications for classically applied ESL statistics. The observed negative correlation between components hints that return levels based on classical ESL statistics may be overestimated. However, it is important to emphasise that these negative correlations are based on the statistics of all values exceeding 99.7 percentile. Furthermore, as we have already described, the negative correlation can be an artefact of the decomposition approach (section 3.1.1). It is commonly assumed that the ESL distributions can be described by either the Generalised Extreme Value (GEV) distribution or the Generalised Pareto Distribution (GPD Coles et al., 2001). However, as, for example, Suursaar and Sooäär (2007) note, some outliers do not fit these distributions. Kudryavtseva et al. (2021) suggest that these 'outliers' could be caused

by a sequence of storms that initially increase the filling state of the Baltic Sea and then create a surge on top of it. Our results show that, on average, the opposite is the case, making these 'outliers' stand out even more. Historical ESL events, such as the 2005 (Suursaar and Sooäär, 2007; Mäll et al., 2017) or the 1872 surge (e.g. Hofstede and Hamann, 2022; Andrée et al., 2023), were a superposition of extremely high filling (71 cm at Landsort, up to 100 cm in the Western Baltic Sea for 1872 and >70 cm for 2005) and an exceptional surge. MacPherson et al. (2023) argue for the inclusion of these historical events, as they substantially influence (increase) the design sea levels. This is particularly important for the Western Baltic Sea, where the ESL activity has been relatively low over the last 70 years, which is the basis for current ESL statistics and design levels (MacPherson et al., 2023).

Note that none of the statistical approaches mentioned have considered the temporal decomposition of the low and high frequency contributions or the interdependence between different components. If the statistics of two (or more) components were considered independently, the peak sea level resulting from the summation of the sea levels of the components with the same return period (the same probability) would be overestimated, because correlations between the components are neglected. Comparing the 95th percentile of the filling component with the mean filling during the ESL events considered in this study (Fig. 10) highlights a key point: the mean filling during ESL events consistently exceeds this percentile threshold across the entire Baltic Sea. This demonstrates a clear coupling between high filling levels and surges, suggesting that a combined statistical distribution, as is traditionally used, remains preferable. However, as discussed in the previous paragraph, this approach may not accurately reflect historical events.

Incorporating the correlations between the three temporal components using copula statistics could enhance the statistical representation of ESLs in the Baltic Sea. This method may help reducing uncertainties in the tail ends of ESL distributions, which are a major source of error when determining design levels for coastal protection. To the best of our knowledge, this approach has not yet been applied to ESLs in the Baltic Sea region.

4.3 Consequences for numerical modelling and climate projections

The clear and dominant importance of winds for the generation of ESLs in the Baltic Sea is expected from physics but poses a problem for numerical ocean models. Since the uncertainty of the storm systems in the atmospheric data is related to the uncertainties in the representation of ESLs in the ocean models (Lorenz and Gräwe, 2023a), the models depend on good atmospheric data.

This poses a significant challenge in estimating how ESLs will respond to climate change in the region. Hindcast simulations demonstrate a wide variation in ESL statistics, even when using an ensemble approach (Lorenz and Gräwe, 2023a). The uncertainty is further compounded by the unpredictable evolution of storm tracks and storm intensities, making future projection even more uncertain (see the recent Baltic Earth Assessment Reports and references therein, e.g. Meier et al., 2022a, b; Rutgersson et al., 2022; Weisse et al., 2021). Therefore, the current state of knowledge is that the storm statistics will most likely stay the same in the future Meier et al. (2022b), since there is no robust change in storms in current regional climate models for the Baltic Sea region. However, it is certain that sea ice cover will decrease in the future and the mean sea level will rise (Fox-Kemper et al., 2021; Gräwe et al., 2019). The latter will raise the extreme value statistics to higher baseline levels
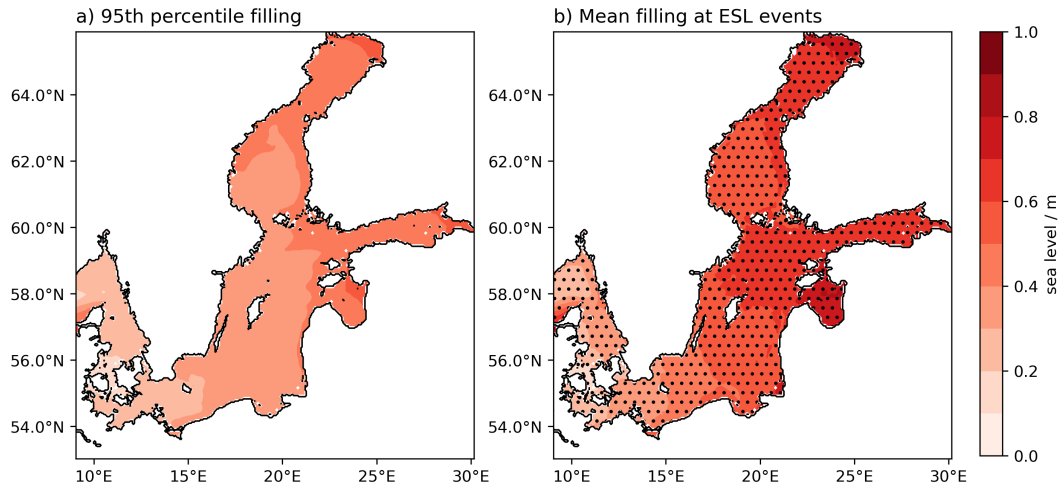
Figure 10. Comparison of the 95th percentile of the filling component (a) to the mean filling component during the ESL events (b). The hashed area indicates, where the mean filling during the ESL events is higher than the 95th percentile in a).

(Wahl et al., 2017; Hieronymus et al., 2018). For shallow lagoon systems, such as those in the western and southern Baltic Sea, sea-level rise will alter water exchange with the Baltic Sea, most likely increasing ESLs there (Lorenz et al., 2023). For the former, increasing ESLs would be expected where sea ice is currently present, e.g. in the Gulf of Bothnia and the Gulf of Finland.

440   Since future ESL statistics are likely to stay the same, except for higher base levels due to sea level rise and the retreat of sea ice cover, future efforts may be directed towards a better understanding of the current distribution and dynamics of ESLs in the Baltic Sea region. This statement applies to physics, e.g. interactions of the different low and high-frequency components and their statistical dependencies.

5   Summary and Conclusions

445   We decomposed observed and numerically modelled extreme sea level (ESL) events in the Baltic Sea into three distinct temporal components: the low-frequency filling of the basin (preconditioning), storm surges, and basin-wide inertial oscillations, known as seiches. Our findings indicate that the surge component is the dominant contributor in the Western Baltic Sea, while the filling component plays the primary role in the central and northern parts of the basin. Although seiches contribute the least, they remain a non-negligible factor.

450   Through numerical simulations, we further examined the driving forces behind each temporal component. Wind emerged as the primary driver for all components, followed by atmospheric pressure. Atlantic sea levels significantly influence the surge component in the Kattegat and Skagerrak regions, located outside the Baltic Sea. However, the Atlantic sea level primarily

affects the filling component within the Baltic Sea. Sea ice was found to impact only the surge component in the northern Baltic Sea, while interannual variations in sea ice, salinity, and temperature had no substantial influence on any of the components.

455   The decomposition framework introduced in this study provides a novel and practical approach for isolating the temporal components and their respective driving forces contributing to ESL events in a non-tidal, semi-enclosed basin like the Baltic Sea. Depending on data availability, this method can be easily adapted for other regions, incorporating additional factors like tides in tidal systems or wave setup. Our framework is valuable for advancing the global understanding of sea level extremes and enhancing coastal risk management strategies.

References

Andrée, E., Su, J., Dahl Larsen, M. A., Drews, M., Stendel, M., and Skovgaard Madsen, K.: The role of preconditioning for extreme storm surges in the western Baltic Sea, Natural Hazards and Earth System Sciences, 23, 1817–1834, https://doi.org/10.5194/nhess-23-1817-2023, 2023.

Arns, A., Wahl, T., Haigh, I., Jensen, J., and Pattiaratchi, C.: Estimating extreme water level probabilities: A comparison of the direct methods and recommendations for best practise, Coastal Engineering, 81, 51–66, https://doi.org/10.1016/j.coastaleng.2013.07.003, 2013.

Arns, A., Wahl, T., Wolff, C., Vafeidis, A. T., Haigh, I. D., Woodworth, P., Niehüser, S., and Jensen, J.: Non-linear interaction modulates global extreme sea levels, coastal flood exposure, and impacts, Nature Communications, 11, 1–9, https://doi.org/10.1038/s41467-020-15752-5, 2020.

Bierstedt, S. E., Hünicke, B., and Zorita, E.: Variability of wind direction statistics of mean and extreme wind events over the Baltic Sea region, Tellus A: Dynamic Meteorology and Oceanography, 67, 29 073, https://doi.org/10.3402/tellusa.v67.29073, 2015.

Bilskie, M. V., Hagen, S. C., Medeiros, S. C., and Passeri, D. L.: Dynamics of sea level rise and coastal flooding on a changing landscape, Geophysical Research Letters, 41, 927–934, https://doi.org/10.1002/2013GL058759, 2014.

Burchard, H. and Bolding, K.: GETM: A General Estuarine Transport Model; Scientific Documentation, European Commission, Joint Research Centre, Institute for Environment and Sustainability, 2002.

Coles, S., Bawa, J., Trenner, L., and Dorazio, P.: An introduction to statistical modeling of extreme values, Springer, https://doi.org/10.1007/978-1-4471-3675-0, 2001.

Fox-Kemper, B., Hewitt, H., Xiao, C., Aðalgeirsdóttir, G., Drijfhout, S., Edwards, T., Golledge, N., Hemer, M., Kopp, R., Krinner, G., Mix, A., Notz, D., Nowicki, S., Nurhati, I., Ruiz, L., Sallée, J.-B., Slangen, A., and Yu, Y.: Ocean, Cryosphere and Sea Level Change. In Climate Change 2021: The Physical Science Basis. Contribution of Working Group I to the Sixth Assessment Report of the Intergovernmental Panel on Climate Change, Cambridge University Press, https://doi.org/10.1017/9781009157896.011, 2021.

Gräwe, U. and Burchard, H.: Storm surges in the Western Baltic Sea: the present and a possible future, Climate Dynamics, 39, 165–183, https://doi.org/10.1007/s00382-011-1185-z, 2012.

Gräwe, U., Naumann, M., Mohrholz, V., and Burchard, H.: Anatomizing one of the largest saltwater inflows into the Baltic Sea in December 2014, Journal of Geophysical Research: Oceans, 120, 7676–7697, https://doi.org/10.1002/2015JC011269, 2015.

Gräwe, U., Klingbeil, K., Kelln, J., and Dangendorf, S.: Decomposing mean sea level rise in a semi-enclosed basin, the Baltic Sea, Journal of Climate, 32, 3089–3108, https://doi.org/10.1175/jcli-d-18-0174.1, 2019.

Groll, N., Gaslikova, L., and Weisse, R.: Recent Baltic Sea Storm Surge Events From A Climate Perspective, EGUsphere, 2024, 1–25, https://doi.org/10.5194/egusphere-2024-2664, 2024.

Haigh, I. D., Marcos, M., Talke, S. A., Woodworth, P. L., Hunter, J. R., Hague, B. S., Arns, A., Bradshaw, E., and Thompson, P.: GESLA Version 3: A major update to the global higher-frequency sea-level dataset, Geoscience Data Journal, https://doi.org/10.31223/x5mp65, 2022.

Heinrich, P., Hagemann, S., Weisse, R., Schrum, C., Daewel, U., and Gaslikova, L.: Compound flood events: analysing the joint occurrence of extreme river discharge events and storm surges in northern and central Europe, Natural Hazards and Earth System Sciences, 23, 1967–1985, https://doi.org/10.5194/nhess-23-1967-2023, 2023.

Hendry, A., Haigh, I. D., Nicholls, R. J., Winter, H., Neal, R., Wahl, T., Joly-Laugel, A., and Darby, S. E.: Assessing the characteristics and drivers of compound flooding events around the UK coast, Hydrology and Earth System Sciences, 23, 3117–3139, https://doi.org/10.5194/hess-23-3117-2019, 2019.

Hersbach, H., Bell, B., Berrisford, P., Hirahara, S., Horányi, A., Muñoz-Sabater, J., Nicolas, J., Peubey, C., Radu, R., Schepers, D., et al.: The ERA5 global reanalysis, Quarterly Journal of the Royal Meteorological Society, 146, 1999–2049, https://doi.org/10.1002/qj.3803, 2020.

Hieronymus, M., Dieterich, C., Andersson, H., and Hordoir, R.: The effects of mean sea level rise and strengthened winds on extreme sea levels in the Baltic Sea, Theoretical and Applied Mechanics Letters, 8, 366–371, https://doi.org/10.1016/j.taml.2018.06.008, 2018.

Hofstede, J. and Hamann, M.: The 1872 catastrophic storm surge at the Baltic Sea coast of Schleswig-Holstein; lessons learned?, Die Küste, https://doi.org/10.18171/1.092101, 2022.

Idier, D., Bertin, X., Thompson, P., and Pickering, M. D.: Interactions between mean sea level, tide, surge, waves and flooding: mechanisms and contributions to sea level variations at the coast, Surveys in Geophysics, 40, 1603–1630, https://doi.org/10.1007/s10712-019-09549-5, 2019.

Kiesel, J., Honsel, L. E., Lorenz, M., Gräwe, U., and Vafeidis, A. T.: Raising dikes and managed realignment may be insufficient for maintaining current flood risk along the German Baltic Sea coast, Communications Earth & Environment, 4, 433, https://doi.org/10.1038/s43247-023-01100-0, 2023a.

Kiesel, J., Lorenz, M., König, M., Gräwe, U., and Vafeidis, A. T.: Regional assessment of extreme sea levels and associated coastal flooding along the German Baltic Sea coast, Natural Hazards and Earth System Sciences, 23, 2961–2985, https://doi.org/10.5194/nhess-23-2961-2023, 2023b.

Kiesel, J., Wolff, C., and Lorenz, M.: Brief communication: From modelling to reality – flood modelling gaps highlighted by a recent severe storm surge event along the German Baltic Sea coast, Natural Hazards and Earth System Sciences, 24, 3841–3849, https://doi.org/10.5194/nhess-24-3841-2024, 2024.

Kirezci, E., Young, I. R., Ranasinghe, R., Muis, S., Nicholls, R. J., Lincke, D., and Hinkel, J.: Projections of global-scale extreme sea levels and resulting episodic coastal flooding over the 21st Century, Scientific reports, 10, 11 629, https://doi.org/10.1038/s41598-020-67736-6, 2020.

Knutson, T. R., McBride, J. L., Chan, J., Emanuel, K., Holland, G., Landsea, C., Held, I., Kossin, J. P., Srivastava, A., and Sugi, M.: Tropical cyclones and climate change, Nature geoscience, 3, 157–163, https://doi.org/10.1038/ngeo779, 2010.

Kudryavtseva, N., Soomere, T., and Männikus, R.: Non-stationary analysis of water level extremes in Latvian waters, Baltic Sea, during 1961–2018, Natural Hazards and Earth System Sciences, 21, 1279–1296, https://doi.org/10.5194/nhess-21-1279-2021, 2021.

Leppäranta, M. and Myrberg, K.: Physical oceanography of the Baltic Sea, Springer Science & Business Media, https://doi.org/10.1007/978-3-540-79703-6, 2009.

Longuet-Higgins, M. and Stewart, R.: Radiation stresses in water waves; a physical discussion, with applications, Deep Sea Research and Oceanographic Abstracts, 11, 529–562, https://doi.org/10.1016/0011-7471(64)90001-4, 1964.

Lorenz, M. and Gräwe, U.: Uncertainties and discrepancies in the representation of recent storm surges in a non-tidal semi-enclosed basin: a hindcast ensemble for the Baltic Sea, Ocean Science, 19, 1753–1771, https://doi.org/10.5194/os-19-1753-2023, 2023a.

Lorenz, M. and Gräwe, U.: [Data set] Results of the study "Uncertainties and discrepancies in the representation of recent storm surges in a non-tidal semi-enclosed basin: a hind-cast ensemble for the Baltic Sea" in Ocean Science, https://doi.org/10.5281/zenodo.8340649, 2023b.

Lorenz, M. and Gräwe, U.: [Data set] Results of the study "Untangling the Waves: Decomposing Extreme Sea Levels in a non-tidal basin, the Baltic Sea", https://doi.org/10.5281/zenodo.13903910, 2024.

Lorenz, M., Arns, A., and Gräwe, U.: How Sea Level Rise May Hit You Through the Backdoor: Changing Extreme Water Levels in Shallow Coastal Lagoons, Geophysical Research Letters, 50, e2023GL105 512, https://doi.org/10.1029/2023GL105512, e2023GL105512 2023GL105512, 2023.

Luomaranta, A., Ruosteenoja, K., Jylhä, K., Gregow, H., Haapala, J., and Laaksonen, A.: Multimodel estimates of the changes in the Baltic Sea ice cover during the present century, Tellus A: Dynamic Meteorology and Oceanography, 66, 22 617, https://doi.org/10.3402/tellusa.v66.22617, 2014.

MacPherson, L. R., Arns, A., Fischer, S., Méndez, F. J., and Jensen, J.: Bayesian extreme value analysis of extreme sea levels along the German Baltic coast using historical information, Natural Hazards and Earth System Sciences, 23, 3685–3701, https://doi.org/10.5194/nhess-23-3685-2023, 2023.

Madsen, K. S., Høyer, J. L., Fu, W., and Donlon, C.: Blending of satellite and tide gauge sea level observations and its assimilation in a storm surge model of the North Sea and Baltic Sea, Journal of Geophysical Research: Oceans, 120, 6405–6418, https://doi.org/10.1002/2015JC011070, 2015.

Mäll, M., Suursaar, Ü., Nakamura, R., and Shibayama, T.: Modelling a storm surge under future climate scenarios: case study of extratropical cyclone Gudrun (2005), Natural Hazards, 89, 1119–1144, https://doi.org/10.1007/s11069-017-3011-3, 2017.

Männikus, R., Soomere, T., and Kudryavtseva, N.: Identification of mechanisms that drive water level extremes from in situ measurements in the Gulf of Riga during 1961-2017, Continental Shelf Research, 182, 22–36, https://doi.org/10.1016/j.csr.2019.05.014, 2019.

McGranahan, G., Balk, D., and Anderson, B.: The rising tide: assessing the risks of climate change and human settlements in low elevation coastal zones, Environment and urbanization, 19, 17–37, https://doi.org/10.1177/0956247807076960, 2007.

Meier, H. E. M., Dieterich, C., Gröger, M., Dutheil, C., Börgel, F., Safonova, K., Christensen, O. B., and Kjellström, E.: Oceanographic regional climate projections for the Baltic Sea until 2100, Earth System Dynamics, 13, 159–199, https://doi.org/10.5194/esd-13-159-2022, 2022a.

Meier, H. E. M., Kniebusch, M., Dieterich, C., Gröger, M., Zorita, E., Elmgren, R., Myrberg, K., Ahola, M. P., Bartosova, A., Bonsdorff, E., Börgel, F., Capell, R., Carlén, I., Carlund, T., Carstensen, J., Christensen, O. B., Dierschke, V., Frauen, C., Frederiksen, M., Gaget, E., Galatius, A., Haapala, J. J., Halkka, A., Hugelius, G., Hünicke, B., Jaagus, J., Jüssi, M., Käyhkö, J., Kirchner, N., Kjellström, E., Kulinski, K., Lehmann, A., Lindström, G., May, W., Miller, P. A., Mohrholz, V., Müller-Karulis, B., Pavón-Jordán, D., Quante, M., Reckermann, M., Rutgersson, A., Savchuk, O. P., Stendel, M., Tuomi, L., Viitasalo, M., Weisse, R., and Zhang, W.: Climate change in the Baltic Sea region: a summary, Earth System Dynamics, 13, 457–593, https://doi.org/10.5194/esd-13-457-2022, 2022b.

Moftakhari, H., Muñoz, D. F., Akbari Asanjan, A., AghaKouchak, A., Moradkhani, H., and Jay, D. A.: Nonlinear Interactions of Sea-Level Rise and Storm Tide Alter Extreme Coastal Water Levels: How and Why?, AGU Advances, 5, e2023AV000 996, https://doi.org/10.1029/2023AV000996, e2023AV000996 2023AV000996, 2024.

Monserrat, S., Vilibić, I., and Rabinovich, A. B.: Meteotsunamis: atmospherically induced destructive ocean waves in the tsunami frequency band, Natural Hazards and Earth System Sciences, 6, 1035–1051, https://doi.org/10.5194/nhess-6-1035-2006, 2006.

Parker, K., Erikson, L., Thomas, J., Nederhoff, K., Barnard, P., and Muis, S.: Relative contributions of water-level components to extreme water levels along the US Southeast Atlantic Coast from a regional-scale water-level hindcast, Natural Hazards, 117, 2219–2248, https://doi.org/10.1007/s11069-023-05939-6, 2023.

Pattiaratchi, C. and Wijeratne, E. M. S.: Observations of meteorological tsunamis along the south-west Australian coast, pp. 281–303,
Springer International Publishing, Cham, https://doi.org/10.1007/978-3-319-12712-5_16, 2015a.

Pattiaratchi, C. B. and Wijeratne, E.: Are meteotsunamis an underrated hazard?, Philosophical Transactions of the Royal Society A: Mathe-
matical, Physical and Engineering Sciences, 373, 20140 377, https://doi.org/10.1098/rsta.2014.0377, 2015b.

Pellikka, H., Laurila, T. K., Boman, H., Karjalainen, A., Björkqvist, J.-V., and Kahma, K. K.: Meteotsunami occurrence in the Gulf of Finland
over the past century, Natural Hazards and Earth System Sciences, 20, 2535–2546, https://doi.org/10.5194/nhess-20-2535-2020, 2020.

Pellikka, H., Šepić, J., Lehtonen, I., and Vilibić, I.: Meteotsunamis in the northern Baltic Sea and their relation to synoptic patterns, Weather
and Climate Extremes, 38, 100 527, https://doi.org/10.1016/j.wace.2022.100527, 2022.

Peltier, W. R.: Global glacial isostasy and the surface of the ice-age Earth: the ICE-5G (VM2) model and GRACE, Annual Review of Earth
and Planetary Sciences, 32, 111–149, https://doi.org/10.1146/annurev.earth.32.082503.144359, 2004.

Pietrzak, J.: The use of TVD limiters for forward-in-time upstream-biased advection schemes in ocean modeling, Monthly Weather Review,
126, 812–830, https://doi.org/10.1175/1520-0493(1998)126<0812:tuotlf>2.0.co;2, 1998.

Pindsoo, K. and Soomere, T.: Basin-wide variations in trends in water level maxima in the Baltic Sea, Continental Shelf Research, 193,
104 029, https://doi.org/10.1016/j.csr.2019.104029, 2020.

Proudman, J.: The Effects on the Sea of Changes in Atmospheric Pressure, Geophysical Supplements to the Monthly Notices of the Royal
Astronomical Society, 2, 197–209, https://doi.org/10.1111/j.1365-246X.1929.tb05408.x, 1929.

Rantanen, M., van den Broek, D., Cornér, J., Sinclair, V. A., Johansson, M. M., Särkkä, J., Laurila, T. K., and Jylhä, K.: The Impact
of Serial Cyclone Clustering on Extremely High Sea Levels in the Baltic Sea, Geophysical Research Letters, 51, e2023GL107 203,
https://doi.org/10.1029/2023GL107203, e2023GL107203 2023GL107203, 2024.

Ridal, M., Olsson, E., Unden, P., Zimmermann, K., and Ohlsson, A.: Uncertainties in Ensembles of Regional Re-Analyses–Deliverable D2.
7 HARMONIE reanalysis report of results and dataset, 2017.

Rueda, A., Vitousek, S., Camus, P., Tomás, A., Espejo, A., Losada, I. J., Barnard, P. L., Erikson, L. H., Ruggiero, P., Reguero, B. G., et al.:
A global classification of coastal flood hazard climates associated with large-scale oceanographic forcing, Scientific Reports, 7, 1–8,
https://doi.org/10.1038/s41598-017-05090-w, 2017.

Rutgersson, A., Kjellström, E., Haapala, J., Stendel, M., Danilovich, I., Drews, M., Jylhä, K., Kujala, P., Larsén, X. G., Halsnæs, K., Lehtonen,
I., Luomaranta, A., Nilsson, E., Olsson, T., Särkkä, J., Tuomi, L., and Wasmund, N.: Natural hazards and extreme events in the Baltic Sea
region, Earth System Dynamics, 13, 251–301, https://doi.org/10.5194/esd-13-251-2022, 2022.

Soomere, T. and Keevallik, S.: Anisotropy of moderate and strong winds in the Baltic Proper, Proc. Estonian Acad. Sci. Eng, 7, 35–49,
https://doi.org/10.3176/eng.2001.1.04, 2001.

Soomere, T. and Pindsoo, K.: Spatial variability in the trends in extreme storm surges and weekly-scale high water levels in the eastern Baltic
Sea, Continental Shelf Research, 115, 53–64, https://doi.org/10.1016/j.csr.2015.12.016, 2016.

Soomere, T., Pindsoo, K., Bishop, S. R., Käärd, A., and Valdmann, A.: Mapping wave set-up near a complex geometric urban coastline,
Natural Hazards and Earth System Sciences, 13, 3049–3061, https://doi.org/10.5194/nhess-13-3049-2013, 2013.

Soomere, T., Eelsalu, M., Kurkin, A., and Rybin, A.: Separation of the Baltic Sea water level into daily and multi-weekly components,
Continental Shelf Research, 103, 23–32, https://doi.org/10.1016/j.csr.2015.04.018, 2015.

Su, J., Murawski, J., Nielsen, J. W., and Madsen, K. S.: Coinciding storm surge and wave setup: A regional assessment of sea level rise
impact, Ocean Engineering, 305, 117 885, https://doi.org/10.1016/j.oceaneng.2024.117885, 2024.

Suursaar, Ü. and Sooäär, J.: Decadal variations in mean and extreme sea level values along the Estonian coast of the Baltic Sea, Tellus A: Dynamic Meteorology and Oceanography, 59, 249–260, https://doi.org/10.1111/j.1600-0870.2006.00220.x, 2007.

Talke, S. A., Familkhalili, R., and Jay, D. A.: The Influence of Channel Deepening on Tides, River Discharge Effects, and Storm Surge, Journal of Geophysical Research: Oceans, 126, e2020JC016 328, https://doi.org/10.1029/2020JC016328, e2020JC016328 2020JC016328, 2021.

Thyng, K. M., Greene, C. A., Hetland, R. D., Zimmerle, H. M., and DiMarco, S. F.: True colors of oceanography: Guidelines for effective and accurate colormap selection, Oceanography, 29, 9–13, https://doi.org/10.5670/oceanog.2016.66, 2016.

Vestøl, O., Ågren, J., Steffen, H., Kierulf, H., and Tarasov, L.: NKG2016LU: a new land uplift model for Fennoscandia and the Baltic Region, Journal of Geodesy, 93, 1759–1779, https://doi.org/10.1007/s00190-019-01280-8, 2019.

Vousdoukas, M., Mentaschi, L., Mongelli, I., Martinez, C., Hinkel, J., Ward, P., Gosling, S., and Feyen, L.: Adapting to rising coastal flood risk in the EU under climate change, EUR 29969 EN, Publications Office of the European Union, Luxembourg, https://doi.org/10.2760/456870, 2020.

Vousdoukas, M. I., Mentaschi, L., Voukouvalas, E., Verlaan, M., Jevrejeva, S., Jackson, L. P., and Feyen, L.: Global probabilistic projections of extreme sea levels show intensification of coastal flood hazard, Nature communications, 9, 1–12, https://doi.org/10.1038/s41467-018-04692-w, 2018.

Wahl, T., Jain, S., Bender, J., Meyers, S. D., and Luther, M. E.: Increasing risk of compound flooding from storm surge and rainfall for major US cities, Nature Climate Change, 5, 1093–1097, https://doi.org/10.1038/nclimate2736, 2015.

Wahl, T., Haigh, I. D., Nicholls, R. J., Arns, A., Dangendorf, S., Hinkel, J., and Slangen, A. B.: Understanding extreme sea levels for broad-scale coastal impact and adaptation analysis, Nature Communications, 8, 1–12, https://doi.org/10.1038/ncomms16075, 2017.

Weisse, R., Dailidienė, I., Hünicke, B., Kahma, K., Madsen, K., Omstedt, A., Parnell, K., Schöne, T., Soomere, T., Zhang, W., and Zorita, E.: Sea level dynamics and coastal erosion in the Baltic Sea region, Earth System Dynamics, 12, 871–898, https://doi.org/10.5194/esd-12-871-2021, 2021.

Wolski, T. and Wiśniewski, B.: Geographical diversity in the occurrence of extreme sea levels on the coasts of the Baltic Sea, Journal of Sea Research, 159, 101 890, https://doi.org/10.1016/j.seares.2020.101890, 2020.

Wolski, T., Wiśniewski, B., Giza, A., Kowalewska-Kalkowska, H., Boman, H., Grabbi-Kaiv, S., Hammarklint, T., Holfort, J., and Lydeikaitė, Ž.: Extreme sea levels at selected stations on the Baltic Sea coast, Oceanologia, 56, 259–290, https://doi.org/10.5697/oc.56-2.259, 2014.

Woodworth, P. L., Hunter, J. R., Marcos, M., Caldwell, P., Menéndez, M., and Haigh, I.: Towards a global higher-frequency sea level dataset, Geoscience Data Journal, 3, 50–59, https://doi.org/10.1002/gdj3.42, 2016.

Wübber, C. and Krauss, W.: The two dimensional seiches of the Baltic Sea, Oceanologica Acta, 2, 435–446, https://archimer.ifremer.fr/doc/00122/23360/, 1979.

Zakharchuk, E. A., Tikhonova, N., Zakharova, E., and Kouraev, A. V.: Spatiotemporal structure of Baltic free sea level oscillations in barotropic and baroclinic conditions from hydrodynamic modelling, Ocean Science, 17, 543–559, https://doi.org/10.5194/os-17-543-2021, 2021.

Zhang, Z. and Leppäranta, M.: Modeling the influence of ice on sea level variations in the Baltic Sea, Geophysica, 31, 31–45, 1995.